







Diurnal and seasonal variation of the elevation gradient of air temperature in the northern flank of the western Qinling Mountain range, China


WANG Guo-yi^{1, 2}  <http://orcid.org/0000-0002-2412-4353>; e-mail: wgy19871119@gmail.com


ZHAO Ming-fei^{1, 2}  <http://orcid.org/0000-0002-3885-2861>; e-mail: Euler_mf@163.com

KANG Mu-yi^{1, 2*}  <http://orcid.org/0000-0003-1010-2433>;  e-mail: kangmy@bnu.edu.cn

XING Kai-xiong^{1, 2}  <http://orcid.org/0000-0001-5621-7848>; e-mail: xingkaixiong@163.com

WANG Yu-hang^{1, 2}  <http://orcid.org/0000-0002-9743-8601>; e-mail: wyhhappy1990@163.com

XUE Feng^{1, 2}  <http://orcid.org/0000-0002-8383-497X>; e-mail: 407495251@qq.com

CHEN Chen³  <http://orcid.org/0000-0002-8340-6115>; e-mail: gene@mail.bnu.edu.cn

* Corresponding author

¹ State Key Laboratory of Earth Surface Processes and Resource Ecology, Beijing Normal University, Beijing 100875, China

² College of Resources Science and Technology, Beijing Normal University, Beijing 100875, China

³ College of Life Sciences, Beijing Normal University, Beijing 100875, China

Citation: Wang GY, Zhao MF, Kang MY, et al. (2017) Diurnal and seasonal variation of the elevation gradient of air temperature in the northern flank of the western Qinling Mountain range, China. *Journal of Mountain Science* 14(1). DOI: 10.1007/s11629-016-4107-z

© Science Press and Institute of Mountain Hazards and Environment, CAS and Springer-Verlag Berlin Heidelberg 2017

Abstract: The typically sparse or lacking distribution of meteorological stations in mountainous areas inadequately resolves temperature elevation variability. This study presented the diurnal and seasonal variations of the elevation gradient of air temperature in the northern flank of the western Qinling Mountain range, which has not been thoroughly evaluated. The measurements were conducted at 9 different elevations between 1710 and 2500 m from August 2014 to August 2015 with HOBO Data loggers. The results showed that the annual temperature lapse rates (TLRs) for T_{mean} , T_{min} and T_{max} were 0.45°C/100m, 0.44°C/100m and 0.40°C/100m, respectively, which are substantially smaller than the often used value of 0.60°C/100m to 0.60°C/100m. The TLRs showed no obvious seasonal variations, except for the maximum temperature lapse rate,

which was steeper in winter and shallower in spring. Additionally, the TLRs showed significant diurnal variations, with the steepest TLR in forenoon and the shallowest in early morning or late-afternoon, and the TLRs changed more severely during the daytime than night time. The accumulated temperature above 0°C, 5°C and 10°C (AT₀, AT₅ and AT₁₀) decreased at a lapse rate of 112.8°C days/100 m, 104.5°C days/100 m and 137.0°C days/100 m, respectively. The monthly and annual mean diurnal range of temperatures (MDRT and ADRT) demonstrated unimodal curves along the elevation gradients, while the annual range of temperature (ART) showed no significant elevation differences. Our results strongly suggest that the extrapolated regional TLR may not be a good representative for an individual mountainside, in particular, where there are only sparse meteorological stations at high elevations.

Received: 26 June 2016

Revised: 30 September 2016

Accepted: 10 October 2016

Keywords: Temperature lapse rate; Temporal variation; HOBO micrologger; Qinling Mountains

Introduction

Mountains account for a large portion of the earth's land surface, and mountain climate is an important component of the earth's climate system. Temperature is undoubtedly the most important aspect of mountain climates, and elevation seems to have the most distinguishing influence on mountain climates (Beniston 2006; Barry 2008). Temperature decreases with increasing elevation, which is widely known as the temperature lapse rate (TLR) and can be predicted from the first principal of earth's atmosphere (Stone and Carlson 1979; Fang and Yoda 1988). An accurate description of the temperature structure over mountain regions is crucial, as it determines the features, direction and speed of many natural processes (Chen et al. 1999; Archer 2004; Minder et al. 2010; Kattel et al. 2013). Mountainous regions are more sensitive to global climate change, the elevation-dependent climatic trends and its important implications on species range shifts (Pepin et al. 2015; Lenoir and Svenning 2015), especially the variation of seasonal and diurnal temperature range (STR and DTR) conclusively affect species elevation range size (Wu et al. 2013; Sheldon and Tewksbury 2014; Chan et al. 2016). All those need to develop climate monitoring along mountain transects that can control for regional heterogeneity (McGuire et al. 2012). However, precise, systematic and long-term in situ measurements on temperature are often unavailable, especially at high-elevated or uninhabited montane regions where there are difficulties in installing and maintaining meteorological instruments (Chiu et al. 2009; Chae et al. 2012).

Due to difficulties in obtaining direct measurements, researchers are usually forced to extrapolate from lowland temperature records using an environmental TLR of $0.65^{\circ}\text{C}/100\text{m}$ or $0.60^{\circ}\text{C}/100\text{m}$ (Prentice et al. 1992; Ngo-Duc et al. 2005; Roe and O'Neal 2009). This value is a spatially global and temporally climatic average that is unsuitable as it may not represent the

atmosphere in specific mountainous regions or in a particular season (Riddering and Queen 2006; Barry and Chorley 2009; Minder et al. 2010). Mountain temperature variability is complicated because it encompasses such a broad range of temporal and spatial scales (Lundquist and Cayan 2007). Many studies based on meteorological stations records (Fang and Yoda 1988; Kattel et al. 2013; Li et al. 2013; Chiu et al. 2014; Guo et al. 2015; Kattel et al. 2015; Li et al. 2015) and observational studies (Tang and Fang 2006; Blandford et al. 2008; Chae et al. 2012) have reported that near-surface TLR shows significant spatiotemporal variability, which differs from region to region depending on the aspect of the slope, location relative to valleys and local climate setting. All of the above mentioned studies emphasized that the mean surface lapse rates differ appreciably from the often-used $0.60^{\circ}\text{C}/100\text{m}$ – $0.65^{\circ}\text{C}/100\text{m}$ values.

Although many studies based on the meteorological stations records have been carried out on the variability of the surface air temperature in mountain regions, most rely on meteorological stations located in the lower elevation range, where the number of weather stations may be insufficient for a complete cover of the altitude and spatial ranges (Rolland 2003; Barry 2008). This may produce biased results because of the scarce distribution in high elevation regions, where research is mostly focused. More complementary case studies are needed to bridge the gap between spatially dense, short-term observations and a sparse network of longer-term observations (Lundquist and Cayan 2007). This is certainly true in the high mountains of western China, where data collected by field instrumentation is still largely lacking. Compared to China's large mountainous area and scope, more attempts are needed to provide detailed transects.

In this paper, we present a systematic arrangement over 800 m elevation ranges in the northern flank of the western Qinling mountain range. An inexpensive and convenient HOBO data logger (Onset, Cape Cod, MA, USA) was used to fulfill this purpose, which is often used by other researchers in mountain regions (Marshall et al. 2007; Pepin et al. 2010; Chae et al. 2012). The objectives of this paper are: (1) to investigate the

diurnal and seasonal variability in temperature and its elevation gradient over this mountain area and (2) to explore the potential controlling factors of these variations.

1 Materials and Methods

1.1 Study Area

The Qinling mountains range extends over 1000 km in central China with an east-west direction, creating a large physical obstacle to advection. It is critical to the distribution of climate and life zones in the eastern part of China (Tang and Fang 2006). The study area is located in the watershed area of the mid-west Qinling Mountain range, where runoffs are divided southward into the Jialing river, then down to the Yangtze river, northward into the Qingjiang river and then to the Wei river, the largest tributary of the Yellow River. Geographically, the study area is between 34°10'N to 34°27'N in latitude and 106°55'E to 107°07'E in longitude, elevating from 1500 to 2500 m a.s.l., approximately 20 km from the Baoji city. The area has a climate with a warm and rainy summer extending through autumn and a cold and dry winter, influenced by both the East Asia and southwest monsoons and the inland continental climates. According to the nearby meteorological observatory Baoji station (107°4'48" E, 34°12'36" N, 612.4 m a.s.l., approximately 6 km from study area), the annual mean temperature (AMT) is 13.5°C and the annual mean precipitation (AMP) is 645.9 mm (Figure 1). Along with the elevation gradient, the vertical vegetation zones distinctively change from coniferous and deciduous broadleaved mixed forest (*Pinus tabulaeformis*, *Pinus armandii* and *Quercus aliena* var. *acuteserrata*, 1600-1800 m),

deciduous broadleaved forests (*Quercus aliena* var. *acuteserrata* forest, 1800-2000 m, and *Betula albo-sinensis* forest, 2200-2400 m), and coniferous forest (*Abies fargesii*, 2400-2500 m) to montane bamboo shrub (*Fargesia nitida*, >2500 m)(Han et al. 2010; Tan 2011).

1.2 Field instrumentation and data collection

To obtain vertical temperature profiles, we installed 9 portable HOBO Pro v2 U23-002 data loggers (Onset, Cape Cod, MA, USA; with temperature range -40°C to 70°C, accuracy of ±0.2°C and resolution of 0.02°C) along the montane slopes with an elevation interval of approximately 100 m from 1710 to 2500 m over the study area (Figure 1). To guarantee the accuracy of the data, the data loggers were checked in an ice water bath before and after measurement, which confirmed their stability and accuracy (deviation from zero ±0.2°C). To keep the ambient environment as constant as possible, all of the data loggers were installed in undisturbed mature forests, far from the forest edge. The data loggers were placed in plastic tubes fixed to the probe and were kept vertically downward, tightened on the

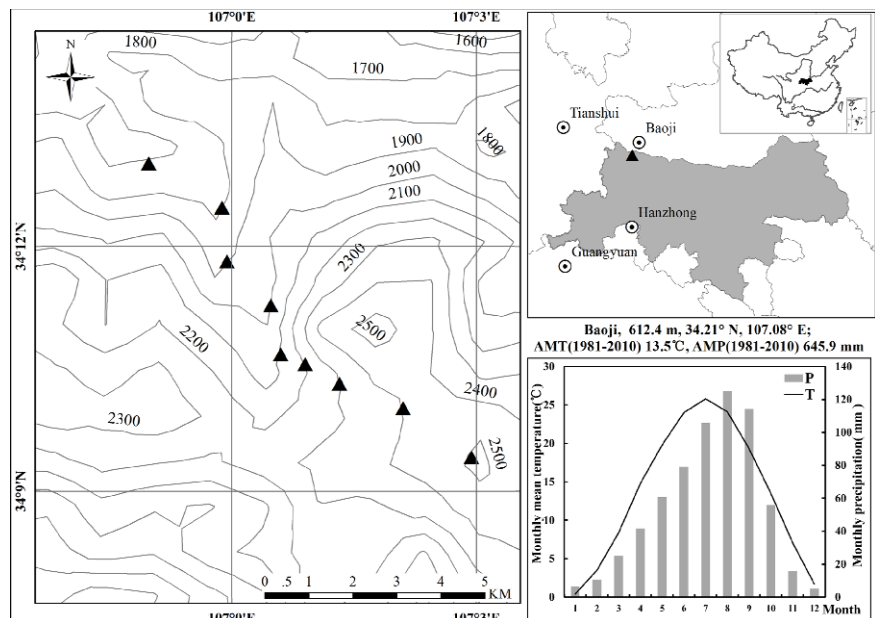


Figure 1 Topography (elevation in m a.s.l.), geographical location, and ecological climate diagram of the study area.

Notes: The ecological climate diagram illustrates the climate characteristic of a nearby meteorological observatory, the Baoji station. AMT: annual mean temperature; AMP: annual mean precipitation.

trunk 1.5 m above the ground with strong zips. All of the data loggers faced toward the northeast side of the trees to eliminate direct solar radiation. The geographic information, including the longitude, latitude and elevation, was also measured using GPS (GARMIN 62sc) and then checked against 1:10 000 DEM maps. To obtain high resolution data, the records were regulated at intervals of 30 min. Therefore, the measurements started at 08:00 on 12 August 2014 and ended at 15:30 on 30 August 2015. We only used the data between 00:00 h on 16 August 2014 and 23:30 h on 15 August 2015 (a whole year) for our analysis.

As a supplementary data source, long-term regional meteorological records were obtained from the meteorological stations surrounding the study area according to the permission granted by the National Meteorological Information Center of China Meteorological Administration (www.nmic.gov.cn). To ensure that all of the meteorological stations were relevant, i.e., within 1° of each other, which was suggested by [Rolland \(2003\)](#) as the largest spatial extent over which the temperature vertical gradient should be expected to remain consistent, we used a buffer analysis in ArcGIS 10.2 according to a 1/2°-radius search to select the potential meteorological stations around the study area. In total, 14 stations were selected, but only 12, which were located in the north face of Qinling mountain range, were used to estimate the regional climatic feature, to be consistent with the study area. These 12 stations were within a latitudinal range of 34.02° to 34.59°N and a longitudinal range of 106.09° to 107.53°E. We used 30 years of annual and monthly records covering the period of 1981 to 2010 to derive the multiyear averages of T_{mean} , T_{max} , and T_{min} at each station.

1.3 Data analyses

To explore the diurnal and seasonal variability in temperature and the elevation gradient, the daily, monthly, seasonal and yearly temperatures were calculated. The daily mean, minimum and maximum temperatures (T_{mean} , T_{min} and T_{max}) were obtained from the observations in one day, and the daily mean temperature was averaged according to 48 records (one record per 30 min). The daily values were aggregated to monthly averages, and the AMT was averaged arithmetically from 12

months. The diurnal range of temperature (DRT) was the difference between the daily maximum and minimum temperatures, and the annual range of temperature (ART) was the difference between the warmest and coldest months. Meanwhile, we calculated three accumulated temperatures (AT₀, AT₅ and AT₁₀) defined as the sum of temperatures for any period in which the daily mean temperature exceeded 0°C, 5°C and 10°C. To explore the diurnal variation of TLR, we also calculated the average temperature for each log point (48 per day) throughout the whole year, and so to each season. The four seasons in a year were divided into spring (March-May), summer (June-August), fall (September-November) and winter (December-February).

A linear regression was used to explore the temperature–elevation relationship due to scarcely any change in longitude and latitude among our observation plots. The coefficient of elevation in linear regression represented the TLR. To compare the present study with long-term regional observations, we also analyzed the relationships between the station-observed temperature and elevation as well as latitude and longitude by using multiple regressions ([Fang and Yoda 1988](#); [Kattel et al. 2013](#)). Additionally, correlation analysis was applied to analyze the effects of climatic factors on the variation of TLRs. TLRs are usually negative because temperature decreases with increasing elevation. We used the terms ‘steeper’ and ‘shallower’ to describe a more negative TLR slope, a less negative or even positive one ([Pepin 2001](#)).

2 Results

2.1 Annual Means

[Figure 2a](#) shows the variation of the mean temperatures with increasing elevation in one year (from 16 of August 2014 to 15 of August 2015). The annual mean of T_{mean} , T_{min} and T_{max} all decreased linearly with increasing elevation. The annual means of T_{mean} , T_{min} and T_{max} were 7.3°C, 4.0°C and 11.1°C, respectively, at 1710 m a.s.l. and declined to 3.6°C, 0.7°C and 7.5°C at 2500 m a.s.l., respectively. The lapse rates of T_{mean} , T_{min} and T_{max} were 0.45°C/100 m, 0.44°C/100 m and 0.40°C/100 m, respectively. The three annual TLRs were very

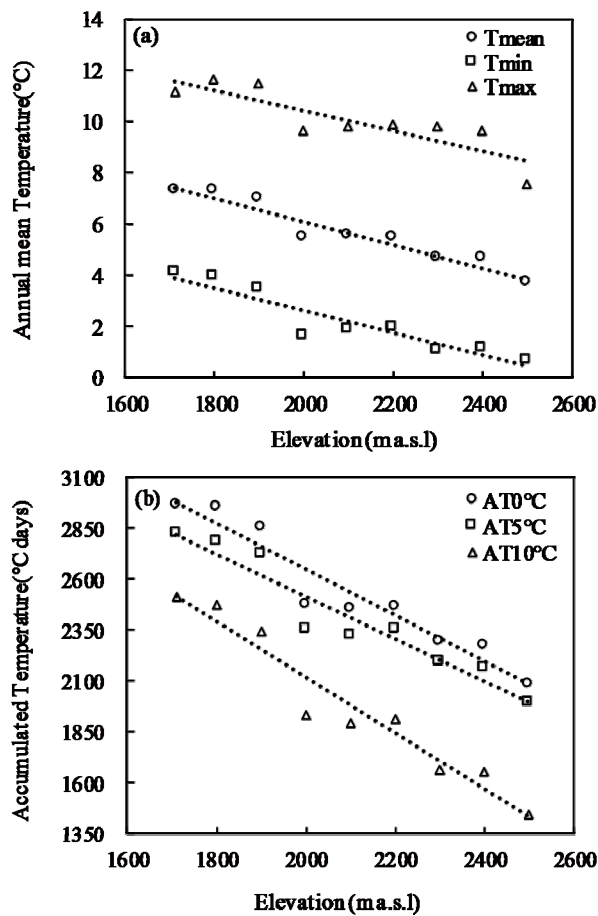


Figure 2 Variations in (a) the annual mean of T_{mean} , T_{min} and T_{max} , (b) the accumulated temperature (AT) above 0°C , 5°C and 10°C in the northern flank of the western Qinling Mountain range.

similar and close to each other, ranging from $0.40^{\circ}\text{C}/100\text{ m}$ to $0.45^{\circ}\text{C}/100\text{ m}$ and agreed well with $0.3^{\circ}\text{C}/100\text{ m}$ – $0.9^{\circ}\text{C}/100\text{ m}$ reported by Fang and Yoda (1988). From our results, the TLR was apparently lower than the generally used value of $0.65^{\circ}\text{C}/100\text{ m}$ or $0.60^{\circ}\text{C}/100\text{ m}$, which further supported the conclusion that the generally used value of TLR is inappropriate in temperate mountain regions. Compared with other researchers' results in Qinling Mountains, the TLRs in our research were shallower than that from Mt Taibai, where TLR was $0.50^{\circ}\text{C}/100\text{ m}$ for AMT by Tang and Fang (2006) and $0.53^{\circ}\text{C}/100\text{ m}$ for few days in summer by Fu et al. (1982). A widely accepted conclusion suggests that TLRs are shallower in humid conditions than that in dry areas (Pepin 2001). Our results are consistent with this conclusion, because the climate is humid in our study area than that in Mt Taibai. This can be

evidenced from the adjacent weather station for the two locations, Baoji station (near to our study area, 107.08°E , 34.21°N , 612.4 m a.s.l.) and the Meixian station (near to Mt Taibai, 107.44°E , 34.16°N , 517.6 m a.s.l.), where the annual precipitation is 645.9 mm and 581.6 mm , respectively.

The accumulated temperature variation of AT₀, AT₅ and AT₁₀ with increasing elevation consistently followed a similar pattern of temperature (Figure 2b). The AT₀, AT₅ and AT₁₀ were 2962.9°C , 2819.9°C and 2511.2°C days, respectively, at 1710 m a.s.l. and decreased to 2079.4°C , 1922.6°C and 1436.2°C days, respectively, at 2500 m a.s.l. . The lapse rate of AT₀, AT₅ and AT₁₀ were $112.8^{\circ}\text{C days}/100\text{ m}$, $104.5^{\circ}\text{C days}/100\text{ m}$ and $137.0^{\circ}\text{C days}/100\text{ m}$, respectively.

2.2 Seasonal changes in temperatures

From the observations made during the study period (16 August 2014 to 15 August 2015), the monthly mean temperature (MMT) was highest in July and lowest in December for all of the elevations assessed in this area. The monthly mean of T_{mean} , T_{min} and T_{max} for July declined from 17.2°C , 13.9°C and 21.7°C , respectively, at 1710 m a.s.l. to 13.7°C , 10.2°C and 18.1°C at 2500 m a.s.l. , respectively. The monthly mean of T_{mean} , T_{min} and T_{max} for December declined from -3.7°C , -7.1°C and 0.2°C , respectively, at 1710 m a.s.l. to -7.5°C , -10.8°C and -4.3°C at 2500 m a.s.l. , respectively (Figure 3a, b, and c). At elevations of 1710 m , 2000 m and 2300 m , a temperature inversion was observed which was defined as the existence of an inversion by the air temperature difference between the higher elevation and adjacent lower observation is greater than 0°C . The inversion frequency is the ratio of inversion occurrence in a certain period. At a lower elevation of 1710 m to 1800 m a.s.l. , the inversion frequency was 38.6% (141 days) throughout the entire year, but more than $2/3$ of them (27.4% , 100 days) were concentrated in the winter period from October to April. At the middle elevation of 2000 m to 2200 m and 2300 m to 2400 m a.s.l. , the inversion frequency was 40.8% (149 days) and 36.2% (132 days), respectively, and smoothly distributed in all seasons (Figure 3d).

The TLR for each month varied with different magnitudes throughout the year (Figure 4a). The

seasonal cycle for the 2014–2015 study period showed different seasonal variations, and the TLRs of T_{mean} and T_{min} did not demonstrate obvious seasonal changes (spring: 0.43; summer: 0.44; autumn: 0.45; and winter: 0.49 for T_{mean} , and spring: 0.43; summer: 0.41; autumn: 0.44; and winter: 0.47 for T_{min} , respectively). For T_{max} , the TLR was steeper in winter (0.51) but shallower in spring (0.29). Additionally, we found larger seasonal amplitudes for TLRs of T_{max} than that for T_{mean} and T_{min} , with a range of 0.38°C/100 m to 0.51 °C/100 m for T_{mean} , 0.35°C/100 m to

0.50°C/100 m for T_{min} and 0.22°C/100 m to 0.53°C/100 m for T_{max} , respectively. Steeper lapse rates for T_{mean} occurred in October with 0.51°C/100m, and shallower lapse rates occurred in June with 0.38°C/100 m. For T_{min} , the values of TLR ranged from 0.35°C/100 m in June to 0.50°C/100 m in November or in January. The TLR of T_{max} ranged from 0.22°C/100 m in May to 0.53°C/100 m in October or in January. The determination the coefficient of R^2 varied for T_{mean} , T_{max} and T_{min} . It seemed there was a stronger and more robust relationship between temperature and

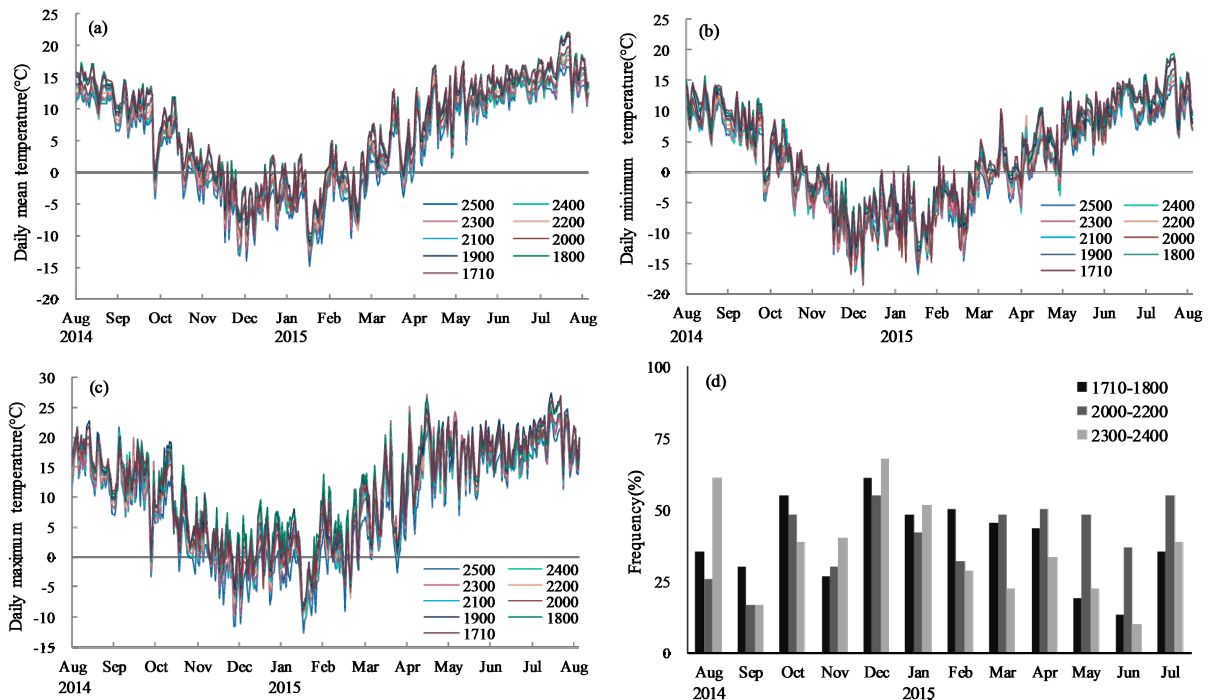


Figure 3 Temporal variations of (a) the daily mean, (b) minimum, (c) maximum air temperature at all elevation sites from 16 August 2014 to 15 August 2015, and (d) the seasonality of the inversion frequency for 1710-1800 m, 2000-2200 m and 2300-2400 m a.s.l. intervals.

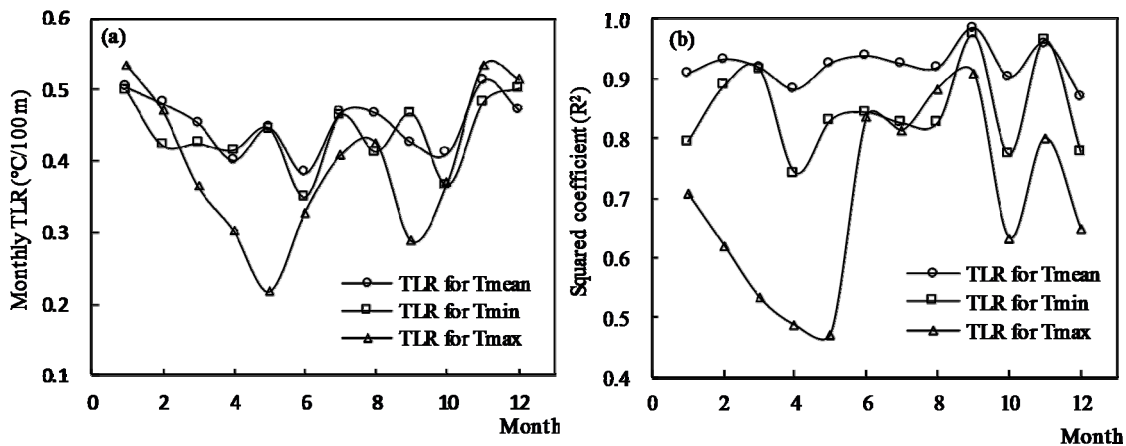


Figure 4 Seasonal variations (a) of the Temperature Lapse Rate (°C/100 m) and squared coefficient (R^2) from linear regression (b) for T_{mean} , T_{min} and T_{max} in the northern flank of the western Qinling Mountain range.

elevation for T_{mean} than for T_{max} and T_{min} . The values of R^2 for T_{max} varied significantly throughout the year, with lower values in spring and higher values in summer (Figure 4b).

2.3 Diurnal changes in temperatures

The average daily temperature variation characteristics at different elevations are shown in Figure 5a. The local time was presented in this paper. It is worth noting that the local time of the study area is 1 hour later than standard Beijing time. The overall trend of daily temperature variation was consistent, warming faster in the daytime and cooling slowly at night. The temperature reached its peak at 12:30-15:00 in the daytime, approximately one hour earlier in the high elevation (2500 m a.s.l., 12:30) than that in other lower elevations, except for the latest peak, which (15:00) occurred at an elevation of 2200 m a.s.l.. The daily lowest temperature was observed at 4:30-5:30 in the early morning. The temperature inversion was also more frequent in the morning (5:00-7:00).

The TLR showed significant diurnal changes during the day and was generally steepest in the forenoon and shallower in the early morning or late-afternoon, with also different diurnal variations in different seasons. Judging from the whole day, the TLR was steepest at forenoon (10:30 a.m.) and shallower in the afternoon (15:30 p.m.) and morning (06:30 a.m.) over a yearly mean (Figure 5b). The largest amplitude of the daily TLR occurred in winter, from 0.38°C/100 m (15:30 p.m.) to 0.60°C/100 m (11:00 a.m.), and the smallest amplitude occurred in autumn, from 0.38°C/100 m (15:30 p.m.) to 0.50°C/100 m (10:00 a.m.). The daily TLR in summer varied at almost the same amplitude as in autumn (from 0.38°C/100 m to 0.51°C/100 m for summer and 0.38°C/100 m to 0.50°C/100 m for autumn). For summer, the shallowest TLR occurred at 6:00 a.m. and steepest at 09:30 a.m.. For autumn, the shallowest TLR occurred at 15:30 a.m. and the steepest occurred at 10:00 a.m. (Figure 5b). To quantify the daytime and nighttime differences of TLR, we determined the day and nighttime span according to the time of sunrise and sunset, and a Wilcoxon rank sum test (a nonparametric test for two independent populations) was performed. The results showed

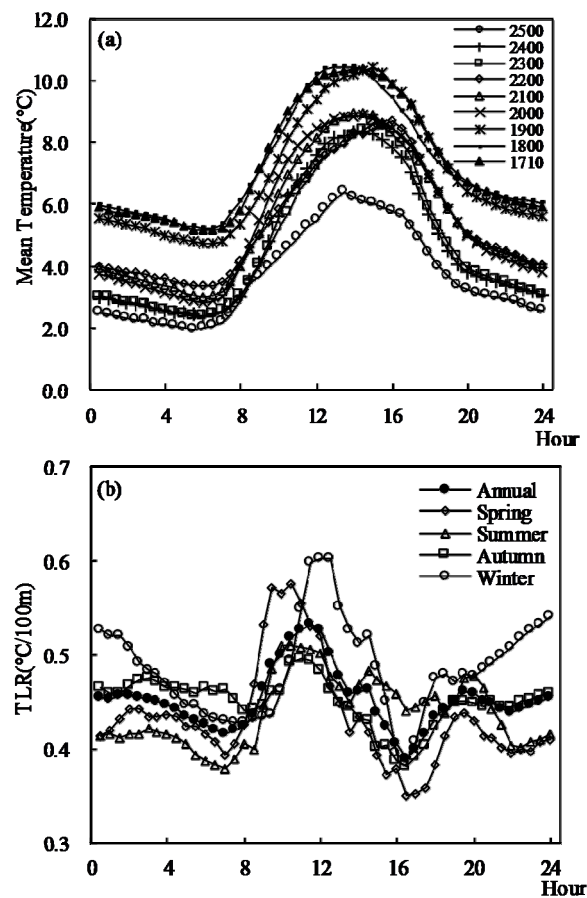


Figure 5 The mean diurnal variation at (a) different elevations and the diurnal variation (b) of the temperature lapse rates (°C/100 m) in the northern flank of the western Qinling Mountain range. Each log lapse rate was an average lapse rate of the same time for different dates from 16 of August 2014 to 15 of July 2015.

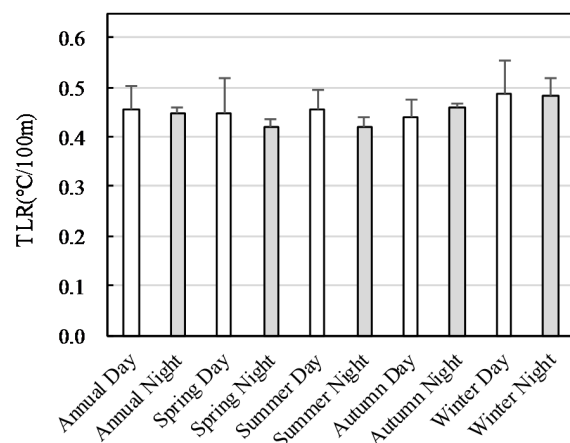


Figure 6 The histograms (bars denote the average TLR +1 standard deviation) of daytime and nighttime TLR (°C/100m) annually and for four seasons in the northern flank of the western Qinling Mountain range.

that the variation (SD) of TLR was larger in the daytime than that in nighttime in all four seasons (Figure 6), and the results showed that the TLR in daytime was significantly different from that in nighttime for summer and autumn ($P < 0.05$).

2.4 Diurnal and annual ranges of temperature

The monthly diurnal range of temperatures (MDRT) demonstrated unimodal curves along the elevation gradients (Figure 7a), fluctuating between 5.8°C (2500 m a.s.l.) and 8.5°C (2400 m a.s.l.) for January and between 7.4°C (1800 m a.s.l.) and 9.0°C (2200 m a.s.l.) for July. The ADRT for the annual mean also showed a unimodal curve, fluctuating between 6.8°C (1710 m a.s.l.) and 8.7°C

(2300 m a.s.l.) (Figure 7a). Seasonally, larger MDRTs were observed in winter and spring (from December to the next May), whereas the smaller MDRTs were observed in September (Figure 7b). The monthly mean temperature for the warmest and the coldest months (ART) exhibited no significant differences along the elevation gradients in the study area.

3 Discussion

3.1 Comparison between long-term observations and the measurements

The most useful data to analyze the relationship between climate and topography is the

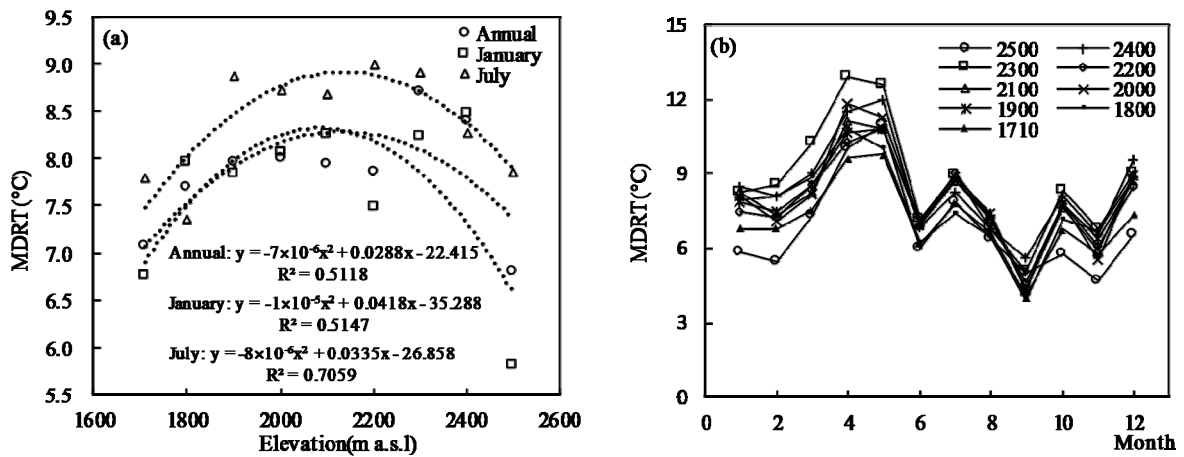


Figure 7 Variation of the monthly diurnal range of temperatures (MDRT) at different elevation (a) and the monthly variation of the average diurnal range of temperatures in the northern flank of the western Qinling Mountain range(b).

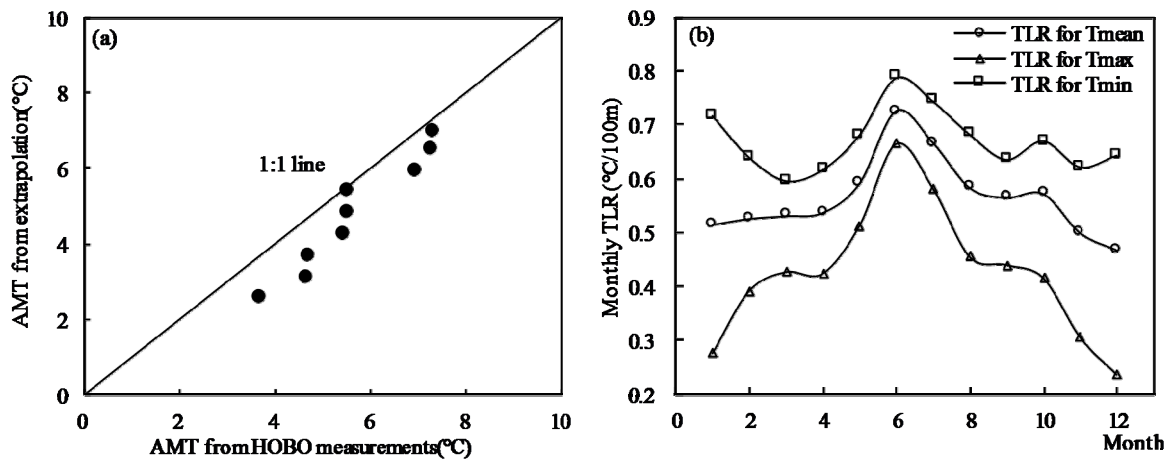


Figure 8 Comparison between the annual mean temperature (AMT) (°C) measured by HOBO loggers and the extrapolated AMT (a); the seasonal variations of TLR (°C/100m) for T_{mean} , T_{min} and T_{max} using multiple regression against long-term observations (b).

long-term meteorological stations records. Here, we analyzed the relationship between station-observed temperature and elevation as well as latitude and longitude by using a multiple regression. The results from the long-term observation TLR for the mean, max and min temperatures are, respectively, $0.568^{\circ}\text{C}/100\text{ m}$, $0.427^{\circ}\text{C}/100\text{ m}$ and $0.669^{\circ}\text{C}/100\text{ m}$ significantly steeper than our short-term record ($0.45^{\circ}\text{C}/100\text{ m}$, $0.40^{\circ}\text{C}/100\text{ m}$, $0.44^{\circ}\text{C}/100\text{ m}$). By using these regional relationships, we compared the calculated AMTs from our observation sites with those extrapolated from the meteorological observatories (Figure 8a). In most elevation cases, our observations were higher than the extrapolated values. Does this mean that using the extrapolated regional TLR to estimate the temperature at high elevation might underestimate the actual local temperature? Meanwhile, the monthly TLR variation was quite different in our observations from the extrapolations derived from the observatory data and was steeper in summer and shallower in winter (Figure 8b).

Therefore, the measurements with the smallest spatial scale of the HOBOS show a weaker correspondence with the surroundings. This may be due to different climates occurring at different elevation locations. The elevation ranges of those selected observatory stations (from 518.4 m to 1665.7 m a.s.l.) for extrapolation are much lower than those of our measurements (from 1710 m to 2500 m a.s.l.) (Li et al. 2015). Additionally, there may be some possible reasons for higher observations than the extrapolated values. Firstly, the present observed TLRs were shallower than long-term observations, resulting in higher values. Secondly, the Mass Elevation Effect (MEE) may have somewhat influence on reshaping the local temperature, because the heating produced by long wave radiation of the mountain surface (the main source of MEE) is more prevalent, then may produce higher temperature than the same elevation from interpolation (Han et al. 2011; Yao et al. 2015). This effect can explain well the higher distribution of tree lines and snowlines in huge mountains of the globe (Han et al. 2011; Zhao et al. 2015). Finally, some other factors, such as climate variation, local topography, soil type, etc., may contribute to this difference. These results may also suggest that on the scale of a mountainside,

the local factors remain important in addition to the regional air mass conditions. This may also highlight that the extrapolated TLR from the regional climate could not be a good representative of the TLR in a particular mountainside location, especially where the elevation is high and the surrounding meteorological stations are rare and sparsely distributed. The regional-scale results should be used with caution when studying features on more local scales (Minder et al. 2010).

3.2 Potential factors controlling the seasonal change of TLRs

The seasonal changes of TLR vary from normally steeper in summer due to the maximum dry convection and shallower in winter due to temperature inversions, as reported by many previous studies. However, a few studies showed other patterns of the seasonal changes of the TLR, such as a reversed pattern (steeper in winter and shallower in summer) in the Qinghai-Tibetan Plateau (Weng and Sun 1984; Guo et al. 2015; Kattel et al. 2015; Li et al. 2015), a bi-modal pattern from the southern slopes of the central Himalayas (Kattel et al. 2013), a pattern that was steeper in winter and shallower in late spring in an Alpine valley (Kirchner et al. 2013), a pattern that was steepest in spring in England (Harding 1978), or even no distinct seasonal change in some regions in China (Li et al. 2013), which contributed to their unique topography and the climate in the regions.

Generally speaking, the TLR is shallower in humid or cooler atmospheric conditions and steeper under dryer or warmer conditions (Pepin 2001; Blandford et al. 2008; Kattel et al. 2013). In our study, the TLR had no obvious seasonal variation; except for the maximum temperature lapse rate. Our results are different from the previous studies in some other mountain regions, as well as from Mt Taibai, which is likely due to the differences in local topography and climatic regimes. To explore the effects of climatic factors on the seasonal change of the monthly TLR, we analyzed the correlations between the TLR and precipitations (a proxy for humidity) as well as cloud cover (a proxy for radiation). The precipitation and cloud cover data were obtained from the closest meteorological observatory, the Baoji station (averaged over the period from 1980

to 2010, Figure 9), where the climate difference was neglected because of its short distance to the study area (approximately 6 km). We found that all of the estimated monthly values of TLR_{mean} , TLR_{max} , and TLR_{min} decreased significantly with the increase of average cloud cover ($r=-0.64$, $P=0.025$ for TLR_{mean} ; $r=-0.81$, $P=0.001$ for TLR_{max} ; and $r=-0.66$, $P=0.02$ for TLR_{min}). A weakly negative relationship between the TLR and monthly precipitation was also detected, though there was no statistical significance ($r=-0.36$, $P=0.25$ for TLR_{mean} ; $r=-0.50$, $P=0.10$ for TLR_{max} ; $r=-0.31$, $P=0.33$ for TLR_{min}).

This meant that both precipitation and cloud cover could influence the TLRs, and the latter was more prominent for TLRs, especially for TLR_{max} . The cloud cover is higher in spring and summer, leading to a significant reduction in insolation during the day (Bhutiyani et al. 2007), thereby reducing TLR_{max} in these seasons. Meanwhile, abundant rainfall in summer and early autumn increase the surface evapotranspiration, thus weakening the elevation-temperature relationship due to the air over high elevations potentially being warmed by the latent heat release associated with water vapor condensation. Thus, we conclude that the seasonal changes of the TLRs on this mountainside might result from a special combination of climatic factors, in particular those with humidity and radiation conditions.

3.3 Potential Causes of the Diurnal variation

The diurnal variation of TLR in our study was a fairly robust characteristic in all four seasons, with steeper lapse rates in the daytime and shallower lapse rates in the early morning or late-afternoon (Figure 5b). This result is consistent with those of other studies, also with Mt Taibai (Tang and Fang 2006), although the magnitude of diurnal variation was different between regions and seasons (Bolstad et al. 1998; Rolland 2003; Minder et al. 2010; Qin et al. 2013). The diurnal differences of TLR might be due to the asymmetric effect of the solar radiation at different elevations (Li et al. 2015). Air temperature at low elevations rises faster than that at high elevations when forced by the same increase of solar radiation due to the admixture with the surrounding atmosphere at

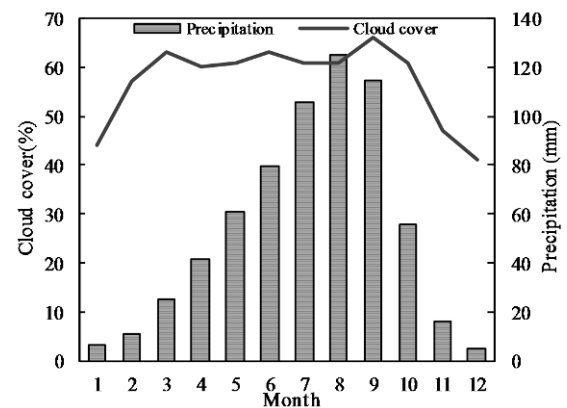


Figure 9 Monthly means of cloud cover (solid black line) and precipitation (bars) at the Baoji station from 1981 to 2010.

high elevations (Barry 2008). That is, the air temperature at high elevation areas was less susceptible to surface heating than at low elevation during the day. Therefore, an increased radiation receipt and asymmetric heating encouraged steeper lapse rates in daytime than nighttime. In addition, the asymmetric radiation cooling effect at different elevations might cause the shallowest TLR to occur at 15:30 in some seasons because the cooling effect at high elevation areas was often faster than that at lower elevation areas due to more prevalent airflow.

The ambient temperatures during the nighttime were less related to the absolute altitude, when the cool and dense air masses tend to fall to low valleys while the relatively warm air masses ascend upward to the slopes (Yoshino 1984; Pepin 1994). This effect of lower TLRs at nighttime caused by nocturnal temperature inversions has already been discussed in several previous studies (Clements et al. 2003; Rolland 2003; Blandford et al. 2008). Moreover, the occurrence of the largest fluctuation amplitude of daily TLR in winter and the smallest in summer might be explained by the seasonal variation of cloud cover, which is lower in winter and higher in summer. The outgoing long wave radiation emitted under clear sky conditions in winter cooled the surface at night, enhancing the difference between the daytime and the nighttime TLRs.

4 Conclusions

Accurate estimate for elevation pattern of temperature in mountain areas is essential for

understanding their ecological process and response to climate change. Based on the HOBO dataloggers records collected over one year from August 2014 to August 2015 at 9 sites in the northern flank of the western Qinling mountain range, we examined and quantified the diurnal and seasonal variations of the elevation temperature gradient, which has not been thoroughly evaluated before. Conclusive results from our study could be drawn as follows: the annual TLRs for T_{mean} , T_{min} and T_{max} were $0.45^{\circ}\text{C}/100\text{ m}$, $0.44^{\circ}\text{C}/100\text{ m}$ and $0.40^{\circ}\text{C}/100\text{ m}$, respectively. The TLRs showed no obvious seasonal variations, except for the maximum temperature lapse rate, which was steeper in winter and shallower in spring. The TLRs showed a significant diurnal variation, and the TLRs changed more severely during the daytime than at nighttime. The characteristics of local TLR displayed a strong relationship with local climatic factors around this area, especially the seasonal changes of cloud cover. As stated above that the elevation pattern of temperature shows large spatiotemporal variation, our results may not

be suitable for other mountainous regions of the world. The significance of our study, however, is in that the expedient assumption of TLR of $0.60^{\circ}\text{C}/100\text{ m}$ - $0.65^{\circ}\text{C}/100\text{ m}$ is a poor one, as well as in that our results may be conducive to developing a pattern of species elevation distribution in the Qinling mountain range.

Acknowledgments

We thank the National Meteorological Information Center of China's meteorological administration (www.nmic.gov.cn) for providing the meteorological observations of surface air temperature, cloud cover and precipitation. This research was funded by the Natural Science Foundation of China (Grant Nos. 41630750, 41271059), and the National Key Basic Research Special Foundation of China (Grant No. 2011FY110300).

References

- Archer D (2004) Hydrological implications of spatial and altitudinal variation in temperature in the upper Indus basin. *Hydrology Research* 35(3): 209-222.
- Barry RG (2008) Mountain weather and climate. Cambridge University Press, Cambridge, U. K.
- Barry RG, Chorley RJ (2009) Atmosphere, weather and climate. Routledge.
- Beniston M (2006) Mountain weather and climate: a general overview and a focus on climatic change in the Alps. *Hydrobiologia* 562(1): 3-16. DOI: [10.1007/s10750-005-1802-0](https://doi.org/10.1007/s10750-005-1802-0)
- Bhutiyan MR, Kale VS, Pawar NJ (2007) Long-term trends in maximum, minimum and mean annual air temperatures across the Northwestern Himalaya during the twentieth century. *Climatic Change* 85(1-2): 159-177. DOI: [10.1007/s10584-006-9196-1](https://doi.org/10.1007/s10584-006-9196-1)
- Blandford TR, Humes KS, Harshburger BJ, et al. (2008) Seasonal and synoptic variations in near-surface air temperature lapse rates in a mountainous basin. *Journal of Applied Meteorology and Climatology* 47(1): 249-261. DOI: [10.1175/2007JAMC1565.1](https://doi.org/10.1175/2007JAMC1565.1)
- Bolstad PV, Swift L, Collins F, et al. (1998) Measured and predicted air temperatures at basin to regional scales in the southern Appalachian mountains. *Agricultural and Forest Meteorology* 91(3): 161-176. DOI: [10.1016/S0168-1923\(98\)00076-8](https://doi.org/10.1016/S0168-1923(98)00076-8)
- Chae H, Lee H, Lee S, et al. (2012) Local variability in temperature, humidity and radiation in the Baekdu Daegan Mountain protected area of Korea. *Journal of Mountain Science* 9(5): 613-627. DOI: [10.1007/s11629-012-2347-0](https://doi.org/10.1007/s11629-012-2347-0)
- Chan WP, Chen IC, Colwell RK, et al. (2016) Seasonal and daily climate variation have opposite effects on species elevational range size. *Science* 351(6280): 1437-1439. DOI: [10.1126/science.aab4119](https://doi.org/10.1126/science.aab4119)
- Chen J, Saunders SC, Crow TR, et al. (1999) Microclimate in forest ecosystem and landscape ecology variations in local climate can be used to monitor and compare the effects of different management regimes. *BioScience* 49(4): 288-297. DOI: [10.2307/1313612](https://doi.org/10.2307/1313612)
- Chiu CA, Lin PH, Lu KC (2009) GIS-based tests for quality control of meteorological data and spatial interpolation of climate data: a case study in mountainous Taiwan. *Mountain Research and Development* 29(4): 339-349. DOI: [10.1659/mrd.00030](https://doi.org/10.1659/mrd.00030)
- Chiu CA, Lin PH, Tsai CY (2014) Spatio-Temporal Variation and Monsoon Effect on the Temperature Lapse Rate of a Subtropical Island. *Terrestrial, Atmospheric & Oceanic Sciences* 25(2): 203-217. DOI: [10.3319/tao.2013.11.08.01\(A\)](https://doi.org/10.3319/tao.2013.11.08.01(A))
- Clements CB, Whiteman CD, Horel JD (2003) Cold-air-pool structure and evolution in a mountain basin: Peter Sinks, Utah. *Journal of Applied Meteorology* 42(6): 752-768. DOI: [10.1175/1520-0450\(2003\)042<0752:CSAEIA>2.0.CO;2](https://doi.org/10.1175/1520-0450(2003)042<0752:CSAEIA>2.0.CO;2)
- Fang JY, Yoda K (1988) Climate and vegetation in China (I). Changes in the altitudinal lapse rate of temperature and distribution of sea level temperature. *Ecological Research* 3(1): 37-51. DOI: [10.1007/BF02348693](https://doi.org/10.1007/BF02348693)
- Fu BP, Yu JM, Li ZY (1982) Characteristics of the summer microclimate in Taibai Mt of Qinling. *Acta Geographica Sinica* 37(01): 88-97. (In Chinese)
- Guo X, Wang L, Tian L (2015) Spatio-temporal variability of vertical gradients of major meteorological observations around the Tibetan Plateau. *International Journal of Climatology* 36(4): 1901-1916. DOI: [10.1002/joc.4468](https://doi.org/10.1002/joc.4468)

- Han F, Zhang BP, Yao YH, et al. (2011) Mass elevation effect and its contribution to the altitude of snowline in the Tibetan Plateau and surrounding areas. *Arctic, Antarctic, and Alpine Research* 43(2): 207-212. DOI: [10.1657/1938-4246-43.2.207](https://doi.org/10.1657/1938-4246-43.2.207)
- Han XH, Wen LF, LIU Y, et al. (2010) Current situation of forest resources and management measures for Matoutan Forestry Bureau. *Shaanxi Forest Science and Technology* (4): 59-61. (In Chinese) DOI: [10.1001-2117\(2010\)04-0059-03](https://doi.org/10.1001-2117(2010)04-0059-03)
- Harding RJ (1978) The variation of the altitudinal gradient of temperature within the British Isles. *Geografiska Annaler. Series A. Physical Geography*: 43-49. DOI: [10.2307/520964](https://doi.org/10.2307/520964)
- Kattel DB, Yao T, Yang K, et al. (2013) Temperature lapse rate in complex mountain terrain on the southern slope of the central Himalayas. *Theoretical and Applied Climatology* 113(3-4): 671-682. DOI: [10.1007/s00704-012-0816-6](https://doi.org/10.1007/s00704-012-0816-6)
- Kattel DB, Yao TD, Yang W, et al. (2015) Comparison of temperature lapse rates from the northern to the southern slopes of the Himalayas. *International Journal of Climatology* 35(15): 4431-4443. DOI: [10.1002/joc.4297](https://doi.org/10.1002/joc.4297)
- Kirchner M, Faus-Kessler T, Jakobi G, et al. (2013) Altitudinal temperature lapse rates in an Alpine valley: trends and the influence of season and weather patterns. *International Journal of Climatology* 33(3): 539-555. DOI: [10.1002/joc.3444](https://doi.org/10.1002/joc.3444)
- Lenoir J, Svenning JC (2015) Climate-related range shifts—a global multidimensional synthesis and new research directions. *Ecography* 38(1): 15-28. DOI: [10.1111/ecog.00967](https://doi.org/10.1111/ecog.00967)
- Li X, Wang L, Chen D, et al. (2013) Near-surface air temperature lapse rates in the mainland China during 1962-2011. *Journal of Geophysical Research-Atmospheres* 118(14): 7505-7515. DOI: [10.1002/jgrd.50553](https://doi.org/10.1002/jgrd.50553)
- Li Y, Zeng Z, Zhao L, et al. (2015) Spatial patterns of climatological temperature lapse rate in mainland China: A multi-time scale investigation. *Journal of Geophysical Research: Atmospheres* 120(7): 2661-2675. DOI: [10.1002/2014JD022978](https://doi.org/10.1002/2014JD022978)
- Lundquist JD, Cayan DR (2007) Surface temperature patterns in complex terrain: Daily variations and long-term change in the central Sierra Nevada, California. *Journal of Geophysical Research: Atmospheres* 112(D11). DOI: [10.1029/2006JD007561](https://doi.org/10.1029/2006JD007561)
- McGuire CR, Nufio CR, Bowers MD, et al. (2012) Elevation-dependent temperature trends in the Rocky Mountain Front Range: changes over a 56- and 20-year record. *Plos One* 7(9): e44370. DOI: [10.1371/journal.pone.0044370](https://doi.org/10.1371/journal.pone.0044370)
- Minder JR, Mote PW, Lundquist JD (2010) Surface temperature lapse rates over complex terrain: Lessons from the Cascade Mountains. *Journal of Geophysical Research-Atmospheres* 115(D14). DOI: [10.1029/2009JD013493](https://doi.org/10.1029/2009JD013493)
- Ngo-Duc T, Polcher J, Laval K (2005) A 53-year forcing data set for land surface models. *Journal of Geophysical Research: Atmospheres* 110(D6). DOI: [10.1029/2004JD005434](https://doi.org/10.1029/2004JD005434)
- Pepin N (2001) Lapse rate changes in northern England. *Theoretical and Applied Climatology* 68(1-2): 1-16. DOI: [10.1007/s007040170049](https://doi.org/10.1007/s007040170049)
- Pepin N, Bradley RS, Diaz HF, et al. (2015) Elevation-dependent warming in mountain regions of the world. *Nature Climate Change* 5(5): 424-430. DOI: [10.1038/nclimate2563](https://doi.org/10.1038/nclimate2563)
- Pepin NC (1994) The possible effects of climate change on the spatial and temporal variation of the altitudinal temperature gradient and the consequences for growth potential in the uplands of northern England. PhD thesis, Durham University.
- Prentice IC, Cramer W, Harrison SP, et al. (1992) Special paper: a global biome model based on plant physiology and dominance, soil properties and climate. *Journal of Biogeography*: 117-134. DOI: [10.2307/2845499](https://doi.org/10.2307/2845499)
- Qin X, Yang XG, Li J, et al. (2013) Analyses on Distribution and Vertical Gradient of Air Temperature on the North Slope of Mt. Qomolangma. *Plateau Meteorology* 32(1): 1-8. DOI: [10.7522/j.issn.1000-0534.2012.00001](https://doi.org/10.7522/j.issn.1000-0534.2012.00001)
- Riddering JP, Queen LP (2006) Estimating near-surface air temperature with NOAA AVHRR. *Canadian Journal of Remote Sensing* 32(1): 33-43. DOI: [10.5589/m06-004](https://doi.org/10.5589/m06-004)
- Roe GH, O'Neal MA (2009) The response of glaciers to intrinsic climate variability: observations and models of late-Holocene variations in the Pacific Northwest. *Journal of Glaciology* 55(193): 839-854. DOI: [10.3189/002214309790152438](https://doi.org/10.3189/002214309790152438)
- Rolland C (2003) Spatial and seasonal variations of air temperature lapse rates in Alpine regions. *Journal of Climate* 16(7): 1032-1046. DOI: [10.1175/1520-0442\(2003\)016<1032:SASVOA>2.0.CO;2](https://doi.org/10.1175/1520-0442(2003)016<1032:SASVOA>2.0.CO;2)
- Sheldon KS, Tewksbury JJ (2014) The impact of seasonality in temperature on thermal tolerance and elevational range size. *Ecology* 95(8): 2134-2143. DOI: [10.1890/13-1703.1](https://doi.org/10.1890/13-1703.1)
- Stone PH, Carlson JH (1979) Atmospheric lapse rate regimes and their parameterization. *Journal of the Atmospheric Sciences* 36(3): 415-423. DOI: [10.1175/1520-0469\(1979\)036<0415:ALRRAT>2.0.CO;2](https://doi.org/10.1175/1520-0469(1979)036<0415:ALRRAT>2.0.CO;2)
- Tan HY (2011). Study on main forest communities structure and their soil properties in the source of Jialing river. Master thesis, Northwest A&F University. (In Chinese)
- Tang ZY, Fang JY (2006) Temperature variation along the northern and southern slopes of Mt. Taibai, China. *Agricultural and Forest Meteorology* 139(3): 200-207. DOI: [10.1016/j.agrformet.2006.07.001](https://doi.org/10.1016/j.agrformet.2006.07.001)
- Weng DM, Sun ZA (1984) A preliminary study of the lapse rate of surface air temperature over mountainous regions of China. *Geographical Research* 3(2): 24-34. (In Chinese)
- Wu Y, Colwell RK, Rahbek C, et al. (2013) Explaining the species richness of birds along a subtropical elevational gradient in the Hengduan Mountains. *Journal of Biogeography* 40(12): 2310-2323. DOI: [10.1111/jbi.12177](https://doi.org/10.1111/jbi.12177)
- Yao YH, Xu M, Zhang BP (2015) Implication of the heating effect of the Tibetan Plateau for mountain altitudinal belts. *Acta Geographica Sinica* 70(3): 407-419. (In Chinese) DOI: [10.11821/dlxb201503005](https://doi.org/10.11821/dlxb201503005)
- Yoshino MM (1984) Thermal belt and cold air drainage on the mountain slope and cold air lake in the basin at quiet, clear night. *GeoJournal* 8(2): 235-250. DOI: [10.1007/BF00446473](https://doi.org/10.1007/BF00446473)
- Zhao F, Zhang BP, Pang Y, et al. (2014) A study of the contribution of mass elevation effect to the altitudinal distribution of timberline in the Northern Hemisphere. *Journal of Geographical Sciences* 24(2): 226-236. DOI: [10.1007/s11442-014-1084-4](https://doi.org/10.1007/s11442-014-1084-4)
- Zhao F, Zhang BP, Zhang S, et al. (2015) Contribution of mass elevation effect to the altitudinal distribution of global treelines. *Journal of Mountain Science* 12(2): 289-297. DOI: [10.1007/s11629-014-3223-x](https://doi.org/10.1007/s11629-014-3223-x)